First-principles studies of the structural and electronic properties of pyrite FeS_2

Joseph Muscat,[1] Andrew Hung,[2] Salvy Russo,[2] and Irene Yarovsky[2]
[1]*CSIRO Minerals, Bayview Avenue, Clayton South, Victoria, 3169, Australia*
[2]*RMIT University, GPO Box 2476V, Melbourne 3001, Victoria, Australia*
(Received 6 September 2000; revised manuscript received 7 May 2001; published 11 January 2002)

We present a study of the structural and electronic properties of Pyrite FeS_2 performed using both localized basis set and plane wave first-principles calculations. Calculations performed using either Gaussian or plane wave basis sets yield results consistent with each other. Small differences in the computed geometries are shown to be due to the choice of pseudopotential employed in the plane wave calculations. The computed densities of states are relatively insensitive to the form of basis set and pseudopotential used. We find that density functional and hybrid approaches predict properties such as geometry and densities of states in good agreement with experiment but that the agreement between the results from Hartree–Fock (HF) calculations and experiment is poor. The reasons for the poor performance of HF theory in this system are examined and are found to be due to the neglect of electronic correlation.

DOI: 10.1103/PhysRevB.65.054107 PACS number(s): 31.15.Ew

I. INTRODUCTION

Metal sulphide minerals are of vast industrial and economic importance. This is because they are the main source of metals such as zinc, copper and lead. In addition, precious metals such as gold and platinum group elements are often associated with the sulphide ores.[1] Sulphides exhibit a wide range of physical, electronic and chemical properties which are under investigation for a range of possible applications including solar cells,[2] solid state batteries[3] and catalysis.

Of the sulphide minerals, pyrite structured FeS_2 is the most common form,[4] and serves as a useful model system for understanding the chemical and physical properties of this class of minerals. Its relatively simple structure, illustrated in Fig. 1, makes it amenable for study using a range of *ab initio* techniques. The chemistry of sulphides, and in particular FeS_2, is of great importance from an environmental perspective since pyrite is a major component of waste material from mining processes. The oxidation and subsequent dissolution of FeS_2 results in the formation of sulphuric acid which causes a significant increase in the acidity of lakes, rivers and streams.[5] This increase of acidity can have an adverse effect on marine wildlife and needs to be carefully monitored and controlled in order to minimize the environmental impact of any mining operation.

There have been a number of recent experimental studies of the bulk and surfaces of pyrite using a wide range of techniques including x-ray photoelectron spectroscopy (XPS),[6,7] low energy electron diffraction (LEED), ultraviolet photoelectron spectroscopy (UPS) and scanning-tunnelling microscopy (STM),[8] inverse ultraviolet photoemission spectroscopy[9,10] and x-ray adsorption spectroscopy.[11] However, in many cases, properties such as the atomic structure of surfaces and interfaces, the nature of defects and the chemistry and energetics of molecular adsorption are difficult, if not impossible, to determine using available experimental techniques.

The increased sophistication of *ab initio* methods coupled with a growth in computer power means that it is now possible to model rather complex physical and chemical systems. Simulation is becoming established as a complementary technique to experiment for the study of minerals as it can provide invaluable primary information on well characterized systems and allows for structural, chemical and stoichiometric effects to be isolated. The additional information provided by simulation can facilitate the interpretation of experimental results. Recent work has demonstrated that computer simulations based on *ab initio* techniques can provide remarkable insights into a diverse range of industrially important systems and processes such as the oxidation of metals[12] and the chemistry of water on catalytically important metal oxides.[13–15]

Most *ab inito* schemes are based on either the Hartree–Fock (HF) approximation, in which electronic exchange is

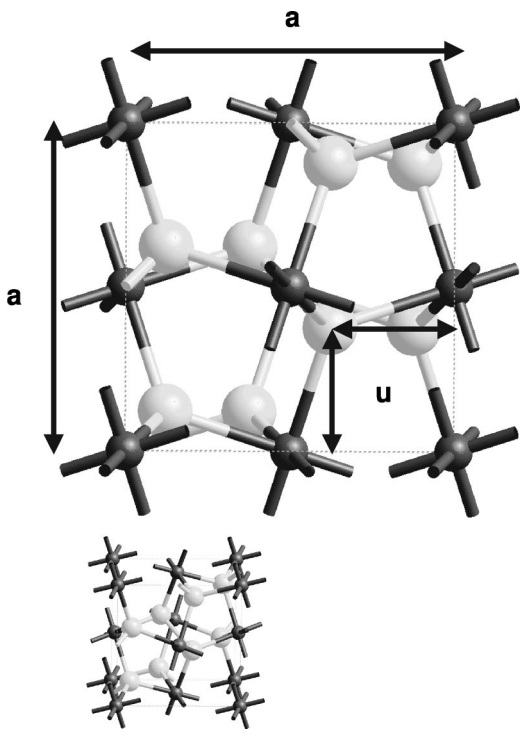

FIG. 1. A bulk unit cell of Pyrite, FeS_2.

treated exactly but correlation effects are neglected and density-functional theory (DFT) in which both exchange and correlation are approximated. In DFT, in the form of the exchange-correlation functional, $E_{XC}[\rho]$ is approximated either using the local density approximation (LDA)[29] or the generalized-gradient approximation (GGA).[33] A number of computational investigations of bulk iron pyrite FeS_2 have been performed using various DFT based methods; these include X_α with LDA;[16] linear muffin-tin orbital atomic sphere aproximation (LMTO-ASA) within the LDA,[17] more recent LMTO-ASA calculations using both the LDA and GGA;[18] pseudopotential-mixed plane wave Gaussian basis LDA and GGA;[19] and full-potential nonorthogonal local-orbital minimum basis band-structure method within the LDA.[20] Calculations of the band structure by these methods predict the Fe^{2+} ion to be in the low-spin, diamagnetic configuration (filled t_{2g} states, empty e_g states), with calculated band gaps in reasonable agreement with experiment varying from around 0.3[19] to 0.85 eV.[20]

Calculations of the optimal cell volume are typically found to be underestimated by LDA, while application of gradient corrections in the form of the GGA tends to overcorrect yielding slightly larger predicted cell volumes[18] with respect to experiment. Studies including geometry optimizations of the pyrite unit cell have tended to result in a predicted S–S bond length greater than the experimentally measured value. Calculated bulk moduli are usually in reasonable qualitative agreement with experiment, with values of about 185 GPa[20] and 165 GPa.[21] A value of 675 GPa (overestimating the experimental value by roughly fourfold) obtained by Temmerman *et al.*[17] has been attributed to the neglect of sulphur coordinate relaxation.

To establish the reliability of the results produced from simulation, it is essential that the theoretical framework as well as the particular computational parameters of the method utilized are tested and validated against experimental results, and can therefore be shown to reliably model the system in question. However, this is often limited by the approximations which are made in different *ab initio* techniques in order to make a calculation computationally tractable. By evaluating what influence some of the different approximations in common use have on the computed properties of the system of interest, it is possible to judge the reliability of a given type of theoretical approximation for predicting a particular set of properties. The level of accuracy and applicability of some of the most common *ab initio* techniques has yet to be quantified for metal sulphide minerals such as FeS_2.

Before undertaking the study of the surface properties and chemistry of pyrite, it is essential to have a good understanding of the bulk material. Hence, in the current work, we seek to further our understanding of the relationship between the electronic structure and the physical and chemical properties of FeS_2. In addition, we seek to determine the reliability of these theoretical techniques and computational parameters as a prerequisite for future studies of the surfaces and interfaces of pyrite. We present the results from one of the first studies using two different *ab inito* methodologies on FeS_2, namely the use of HF and DFT in conjunction with a localized, Gaussian basis set and DFT within the plane wave pseudopotential formalism.

TABLE I. The optimized S^- Gaussian basis set. α_k represents the exponents and C_s, C_p and C_d represent the coefficients of the 4sp, 5sp and 3d functions.

Shell	α_k	C_s	C_p	C_d
4sp	0.280	1.0	1.0	
5sp	0.126	1.0	1.0	
3d	0.300			1.0

II. METHOD

All calculations have been performed using the periodic, linear combination of atomic orbitals (LCAO) formalism as implemented in the CRYSTAL98[22] package and the plane wave pseudopotential technique using the CASTEP[23] software package.

In the LCAO methodology employed within the CRYSTAL98 code, the Bloch orbitals of the crystal are expanded using atom centred Gaussian orbitals with s, p or d symmetry. The main approximation in the current calculations is the choice of the local basis set. Initial attempts to perform a single point energy calculation of bulk FeS_2 at the experimental cell parameters with the Fe basis set from Towler *et al.*[24] and a S basis set used in previous studies of sulphides[25] resulted in convergence problems with hundreds of SCF cycles needed to achieve convergence. Tests revealed that the cause of these problems was due to the S basis set which was optimized for the S^{2-} ion in PbS. The diffuse outer exponents required to describe the S^{2-} ion in galena result in linear convergence problems when used to describe S^- ions in pyrite due, in part to the significantly shorter S–S bond length in FeS_2 compared to PbS. We have used the basis set from Mian *et al.*[25] incorporating *d*-symmetry polarization functions as a starting point and reoptimized the outer 4sp and 5sp exponents with respect to the total energy for the S^- ion in free space before reoptimizing in bulk FeS_2 at the experimental geometry. Using the resulting S^- basis set, for which the reoptimized 4sp and 5sp basis functions are presented in Table I, a single point bulk FeS_2 calculation can be converged in a few tens of SCF cycles. It is more difficult to determine whether a basis set is converged when using localized basis functions as opposed to plane waves. Nonetheless we perfomed tests using an hierarchy of modified Fe and S basis sets incorporating different numbers of valence and d-symmetry functions. Higher angular momentum f- or g-symmetry functions are not available in the CRYSTAL98 code. We found that the Fe basis set from Towler and the modifed S^- basis set described above gave the best compromise between computational expense and accuracy.

A variety of self consistent treatments of exchange and correlation have been used including HF, the LDA to DFT, the GGA to DFT and the B3LYP functional based on Becke's three parameter hybrid functional (B3LYP) employing a combination of HF and DFT exchange.[26] The DFT-LDA calculations were performed using LDA exchange[27] and the

correlation functional parametrized from Monte Carlo calculations[28] by Perdew and Zunger[29] whereas the GGA calculations employed the exchange and correlation functionals by Perdew, Burke and Ernzerhof.[30,31] The B3LYP hybrid functional used in this study is a modified version of Becke's original three-parameter exchange-correlation functional[26] as suggested by Stephens *et al.*[32] where the exchange and correlation is given by

$$E_{\mathrm{XC}}=(1-a_0)E_X^{\mathrm{LDA}}+a_0E_X^{\mathrm{HF}}+a_x\Delta E_X^{\mathrm{B88}}+a_cE_C^{\mathrm{LYP}}+(1-a_c)E_C^{\mathrm{VWN}}, \quad (1)$$

where $a_x\Delta E_X^{\mathrm{B88}}$ is Becke's gradient correction to the exchange functional,[33] and the correlation is given by a combination of the Lee, Yang and Parr (LYP)[34] and the Vosko, Wilk and Nussair[35] functionals. Becke's original three empirical parameters ($a_0=0.2$, $a_x=0.72$, and $a_c=0.81$) are used, which were found to optimize the atomization energies, ionization potentials and proton affinities of a number of small molecules.[26] Solid state calculations using this functional have been shown to yield band gaps in excellent agreement with experiment.[36]

Sampling of K-space has been performed using Pack–Monkhorst grids[22,37] of shrinking parameter 8, yielding 45 symmetry inequivalent K-points for bulk FeS_2. Tests reveal that increasing the number of K-points produces no significant difference in the computed structure or energy of the crystals (the total energy of the bulk crystals is converged to within about 1E−5 eV). CRYSTAL98 computes the matrix elements of the Coulomb and exchange terms by direct summation of the infinite periodic lattice. The truncation of these summations is controlled by five Gaussian overlap criteria; details of the control of these parameters is available elsewhere.[22,38] The values of the overlap criteria chosen in the current study were high (ITOLS parameters set to 10^{-7}, 10^{-7}, 10^{-7}, 10^{-7} and 10^{-14}) in order to converge numerical errors to 1 meV in the total energy.[39] The structural optimizations were converged to a tolerance of 0.01 Å in cell parameters and 10^{-4} eV in the total energy using a modified Broyden–Fletcher–Goldfarb–Shanno (BFGS) minimization algorithm.[40]

CASTEP is based on the DFT framework with the crystalline orbitals expanded in a truncated plane wave basis, incorporating all terms with kinetic energy below a prescribed energy cutoff E_{cut}. The exchange-correlation energy has been computed using functionals based on the LDA parametrized by Perdew–Zunger (as used in the CRYSTAL98 calculations) and GGA functionals by Perdew and Wang.[41] Tests were performed to ensure that lattice parameters and total energy are converged with respect to plane wave cutoff to within the tolerances described in Sec. III. The basis set convergence was checked by performing geometry optimizations using a range of increasing plane wave cutoffs until satisfactory convergence in the geometry and total energy was achieved.

Fe and S core orbitals were removed by applying the frozen-core approximation, whereby a pseudopotential is generated which replaces the core states and incorporates the nucleus as well as the core states as a single entity. Radial nodes present in the original valence orbitals around the core region, which are required for orthonormalization with the core orbitals, are removed producing ''smooth,'' nodeless pseudo-valence orbitals, which reproduce the exact valence orbitals outside a prescribed core cutoff radius r_c. The use of a larger r_c in generating the pseudopotential (thus generating a ''softer'' pseudopotential) allows the use of a lower plane wave cutoff and thus enables more efficient computation. The effects of pseudopotential hardness on FeS_2 structural and electronic properties have been examined by comparing results acquired using Ultrasoft pseudopotentials[42] against those obtained from using Troullier–Martins pseudopotentials.[43] Wave function minimization is achieved by simultaneous all-bands optimization using a conjugate-gradients algorithm. The optimization of the unit cell was performed by minimization of the stress tensor on the cubic supercell through a BFGS[40] scheme. Internal sulphur coordinates were optimized using a conjugate-gradient algorithm. The sampling of the Brillouin zone was performed using the Monkhorst–Pack scheme. Tests were performed to ensure that a sufficient *K*-point density was used for convergence of the lattice parameter and total energy. Fast Fourier transforms (FFT) were used to evaluate matrix elements. The FFT integration mesh is related to the number of basis functions used to describe the crystal, and thus varies according to both plane wave cutoff energy as well as the supercell volume. For cell volume optimizations, the FFT mesh density prescribed is preferably higher than that required for total energy convergence of the initial supercell.

We have calculated the bulk modulus, B, and its derivative, B', of pyrite by fitting the Murnaghan equation of state[44] to the computed energy-volume curve.

III. RESULTS

A. Electronic structure

Experimentally, FeS_2 exists as a diamagnetic mineral with the metal ions in a low-spin Fe^{2+} configuration.[45] We have performed tests to determine the lowest energy electronic structure by performing single point calculations at the experimental geometry with the Fe^{2+} ions converged in either the high-spin (paramagnetic) or low-spin (diamagnetic) states. We find that the LDA, GGA and B3LYP calculations yield a diamagnetic ground state, lower in energy compared to the paramagnetic state by 17.0, 12.3 and 3.90 eV, respectively. However, HF theory predicts the paramagnetic state to be the most stable by 2 eV. These differences are due to correlation effects in Fe^{2+} and will be discussed in Sec. IV.

TABLE II. The charge state of the Fe and S ions (in $|e|$) computed using a Mulliken scheme.

Method	Fe	S
HF	1.66	−0.83
LDA	1.19	−0.59
GGA	1.24	−0.62
B3LYP	1.19	−0.59

We have performed an analysis of the charge on the Fe and S sites using the Mulliken scheme.[46] We note that the partitioning of the charge density among individual atoms is arbitrary and, in the case of the Mulliken analysis, depends on the local basis functions used. In the current calculations the use of a consistent basis set approximation means that variations in the population analysis with functional and structure do provide a useful guide to changes in the nature of the electronic state. The Mulliken charge populations of the Fe and S sites are given in Table II. HF theory yields a charge of $+1.66\,|e|$ on the Fe sites whereas DFT and B3LYP predict pyrite to be far more covalent with a charge on the Fe sites of about $+1.2\,|e|$. The tendency for HF theory to overestimate ionicity has been reported in previous studies of semi-ionic systems such as TiO_2.[47]

The densities of states (DOS) for bulk FeS_2 computed with the HF approximation, DFT and hybrid functionals using CRYSTAL98 are presented in Fig. 2 and the main features of the DOS are summarized in Table III. The valence band is predominantly composed of S 3p and 3d states hybridized with Fe 3d states whereas the conduction band is mainly due to the unoccupied S 3d states (see Fig. 3) in agreement with recent theoretical studies.[48] The two peaks at around 13 to 18 eV correspond to bonding and antibonding S 3s states (Fig. 3) .

The LDA and GGA predict FeS_2 to be a conducting material whereas HF and B3LYP calculations predict a band gap of 11 and 2 eV, respectively. The reason behind the overestimation of the band gap by HF theory arises from a lack of screening in the exchange term leading to an overstabilization of the occupied states. It is also interesting to note that HF theory predicts that the Fe 3d states lie at the bottom of the valence band at around -6 eV whereas LDA, GGA and B3LYP place these states at top of the valence band, about -1 eV. Furthermore, the gap between the bonding and antibonding S 3s states is significantly overestimated by HF theory (4.5 eV) compared with experiment (3 eV); see Table III. Clearly, HF theory yeilds a significantly different electronic structure to the other treatments of exchange and correlation tested. It is of interest to note that Eyert *et al.*,[48] using the augmented spherical wave (ASW) method within the LDA, acquired a computed band gap of 0.95 eV, in almost exact agreement with the current most accurate experimental value (0.95 eV) (see Table III), in contrast to our findings using the LDA. However, it has been found that the computed electronic structure of pyrite (and hence the band gap) can be sensitive to the choice of radii and location of empty muffin-tin spheres within the crystal lattice (see, for example, Eyert *et al.*[48] and Folkerts *et al.*[49]). Their choice of atom-centered and empty sphere radii location, while giving minimum linear overlap between spheres, probably resulted in a computed band gap which is in fortuitous agreement with experiment.

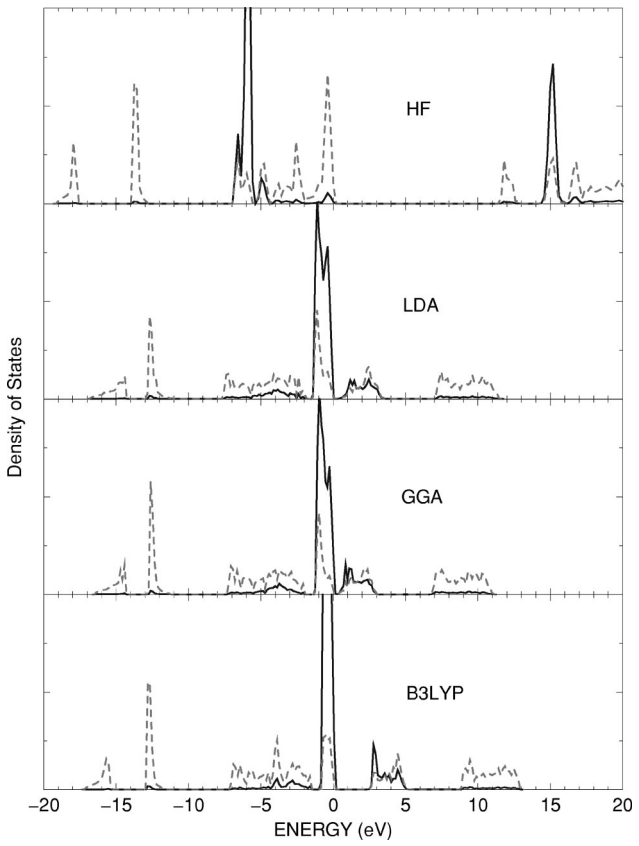

FIG. 2. The computed densities of states of FeS_2 computed using CRYSTAL98 with HF, LDA, GGA and B3LYP treatments of exchange and correlation. Solid lines represent states due to Fe ions, dashed lines represent states due to S ions. The Fermi level has been set to 0 eV and the y-axis is in arbitary units.

The DOS computed with LDA and GGA using CASTEP are presented in Fig. 4. The CASTEP calculations also predict a metallic ground state within the LDA and GGA treatments of exchange and correlation. Peak positions and band widths are in excellent agreement with the results computed using

TABLE III. The positions and widths of the main features (in eV) in the computed densities of states.

Method	Band gap	S 3p width	S 3s σ_b	S 3s σ_a	Fe 3d	S 2p	S 2s
HF	11	7	13.5	18	5.5 - 6.5	171	234
LDA	Conductor	8	12.5	15	0 - 1.5	152	204
GGA	Conductor	7.5	12.5	15	0 - 1.5	152	205
B3LYP	2	7	12.5	15.5	0 - 1	156	211
CASTEP LDA	Conductor	8	12.5	15	0 - 1.5		
CASTEP GGA	Conductor	7.5	12	14.5	0 - 1.5		
LDA-ASW (Ref. 48)	0.95	7.5	13.3	16.4	0 - 1.5		
Expt. (Refs. 6,7,58,65,66)	0.95	6	13	16	0 - 1	162.5	

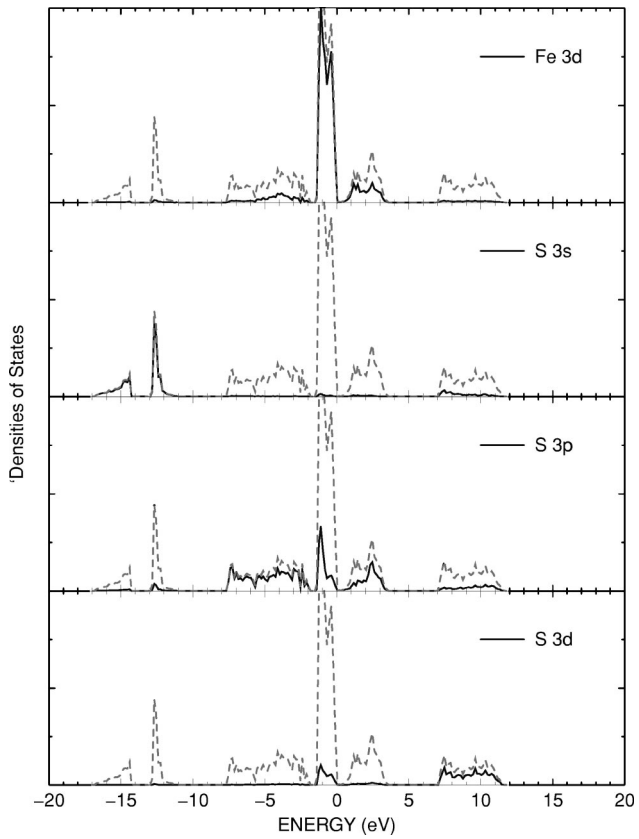

FIG. 3. The projected densities of states for pyrite computed within the LDA. Dashed lines represent the total DOS.

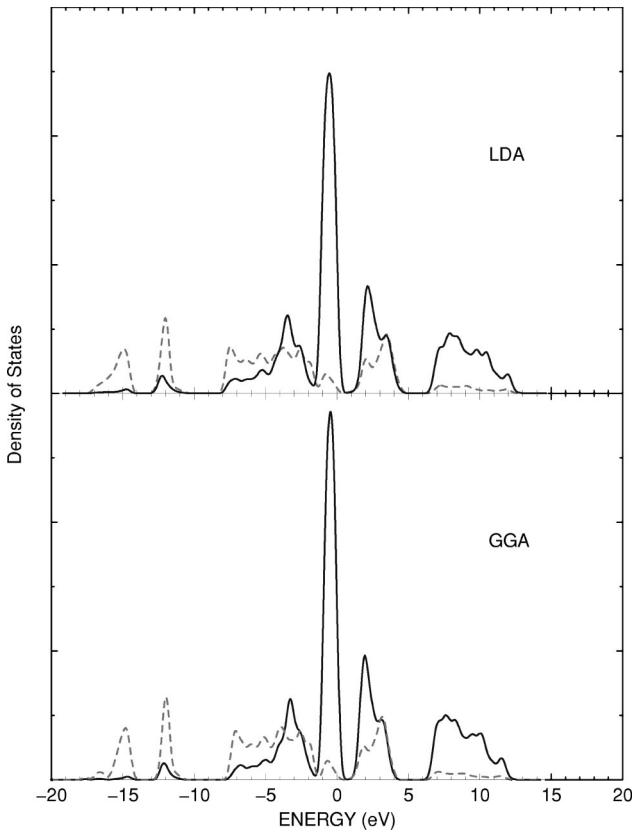

FIG. 4. The densities of states of FeS_2 computed using CASTEP with LDA, GGA treatments of exchange and correlation. Solid lines represent states due to Fe ions, dashed lines represent states due to S ions.

CRYSTAL98 (see Table III) and are in good agreement with experiment.

B. Structural properties

The structure of pyrite FeS_2 is defined by the cell length a_0 and the sulphur internal coordinate, x_s (see Fig. 1). The pyrite structure is cubic, similar to NaCl but with the anions replaced by S_2 dimers with their molecular axes orientated along the four crystallographic $\langle 111 \rangle$ orientations. Each sulphur atom is coordinated to another sulphur atom (the other half of the S_2 dimer) and three Fe atoms. Each Fe atom is coordinated to six sulphurs with equal Fe–S bond distances but the octahedron is compressed along one axis.

The lattice parameters of the optimized structures of FeS_2 as computed using HF, LDA, GGA and B3LYP treatments of exchange and correlation with CRYSTAL98 and with LDA and GGA using CASTEP are presented in Table IV. All the optimized structures presented in Table IV are for FeS_2 in the low-spin diamagnetic state although we note that HF theory yields a paramagnetic ground state for FeS_2. The values of a_0 computed using the CRYSTAL98 code with LDA GGA, and B3LYP treatments of exchange and correlation are in good agreement with experiment, with LDA underestimating by 0.37% and GGA and B3LYP overestimating by 1.9% and 3.7%, respectively. However, the cell volume computed within the HF approximation is in poor agreement with experiment, with an overestimate of over 10%. The reason for the failure of the HF approximation to predict the structure of FeS_2 will be discussed in Sec. IV. Calculations of the cell volumes performed with CASTEP using the LDA yield an underestimate of the cell volume (by 3.1%) while the GGA corrects for this overbinding effect leading to an increased cell volume (although it is still underestimated by 1.0% with respect to experiment). Similar trends were reported in the CRYSTAL98 results.

We have performed tests to check that the cell parameters are converged with respect to the basis set and to determine the influence of the pseudopotential on the computed results. In the case of the CRYSTAL98 calculations, we find that the computed lattice constant is very sensitive to the presence of d-symmetry polarization functions on the sulphur atoms as reported for PbS.[50] Removal of the d-symmetry functions leads to a systematic increase in the cell volume of between 1% and 2% and an increase in the total energy of the system, irrespective of the treatment of exchange and correlation. This suggests that quadrupolar polarization effects must be taken into account in order to yield reliable structural parameters.

With regards to the plane wave CASTEP calculations, tests revealed that when using Ultrasoft pseudopotentials on Fe and S, a plane wave cutoff energy of 400 eV (corresponding to a $27\times27\times27$ FFT mesh) and Monkhorst–Pack k-point grid density of $8\times8\times8$ were sufficient for convergence of the total energy to 0.06 eV/unit cell. These computational

TABLE IV. The computed cell parameters for pyrite. a_0 is the cell parameter in Å and x_s is the internal coordinate in fractional units.

	HF			LDA			GGA			B3LYP		
Method	a_0		x_s	a_0		x_s	a_0		x_s	a_0		x_s
CRYSTAL98	6.000	(10.8)	0.397	5.386	(-0.37)	0.378	5.520	(1.9)	0.380	5.614	(3.7)	0.387
CASTEP				5.247	(-3.1)	0.382	5.360	(-1.0)	0.384			
VASP (Ref. 53)							5.299	(-2.2)	0.383			
Zeng (Ref. 19)				5.441	(0.46)		5.455	(0.72)				
FP (Ref. 20)				5.302	(-2.1)	0.386						
Expt. (Ref. 67)	5.416		0.385									

parameters result in convergence of the lattice parameters to within 0.01 Å for a_0 and 10^{-4} for the internal sulphur coordinate. Using the harder, Troullier–Martins pseudopotentials for Fe and S, an E_{cut} of 890 eV and Monkhorst–Pack grid of $8\times8\times8$ were required for convergence of the total energy, a_0 and x_s to the same tolerance levels.

As noted above, the lattice parameters calculated within the LDA using Ultrasoft pseudopotentials converge to approximately 5.247 Å and 0.3818 for a_0 and x_s, respectively, deviating from the experimental values by -3.3% and -0.83%, respectively. Using the GGA functionals results in lattice parameter values which are in better agreement with experiment (a_0 of 5.360 Å and x_s of 0.3845), studies reducing the discrepancy in the cell volume and internal coordinate to -1.0% and -0.13% with respect to experiment. It can be seen that Ultrasoft pseudopotentials consistently overestimate the Fe-Fe cohesive energy, even with incorporation of gradient corrections. This suggests somewhat poor transferability of the Fe pseudopotential due to inadequate description of the outer-core region as a result of an overly high core cutoff radius. This is further supported by GGA calculations where we performed a cell optimization using the harder Troullier-Martins pseudopotentials. The calculations predicted lattice parameters of 5.478 Å and 0.3847, deviating from experimental values by $+1.14\%$ and -0.08%. This result is consistent with previous findings from GGA calculations on transition metals and transition metal solids, where GGA consistently underestimates the cohesive energy and hence overestimates the cell length.[51] We have found similar trends in lattice parameter variation with pseudopotential hardness from recent plane wave calculations on pure bcc Fe.[52]

The nearest S–S bond distances predicted by the different theories are summarized in Table V. The S–S bond distance computed with CRYSTAL98 using HF and B3LYP are in good agreement with experiment whereas the LDA and GGA bond distances are over 5% too large. Overstimates of the S–S bond distances of a similar magnitude were also reported in recent localized basis set DFT calculations.[19] The current CASTEP results yield S–S bond distances in excellent agreement with experiment and with recent plane wave GGA simulations.[53]

The bulk moduli and their derivatives of FeS_2 computed with CRYSTAL98 using the LDA, GGA, and B3LYP functionals and with CASTEP using the LDA and GGA are presented in Table VI. The CASTEP calculations were performed using Ultrasoft pseudopotentials, other computational parameters for CRYSTAL98 and CASTEP calculations were as described in Sec. II. The bulk moduli predicted by the two programs were almost identical within the LDA yielding a value of around 210 GPa and the GGA giving 164 GPa. This level of agreement is probably somewhat fortunate considering there is a small difference in the computed cell volumes from the two codes. B3LYP yields a lower bulk modulus than DFT, probably due to the overestimate of the cell parameter. The GGA and B3LYP bulk moduli are in reasonable agreement with experimental determinations of around 150 GPa[54–56] although some experiments have measured the bulk modulus to be as high as 215 GPa.[57] The value of the volume derivative of the bulk modulus is significantly harder to determine experimentally (and is often just assumed to be 4) although one experimental study has measured it to be 5.5[57] in good agreement with the current GGA and B3LYP results.

IV. DISCUSSION

We find that plane wave and Gaussian basis set calculations give results consistent with each other with LDA, GGA

TABLE V. The computed S–S bond distances in Å.

Method	HF		LDA		GGA		B3LYP	
CRYSTAL98	2.143	(-0.9)	2.274	(5.2)	2.295	(6.2)	2.197	(1.6)
CASTEP			2.145	(-0.8)	2.154	(-0.4)		
VASP (Ref. 53)					2.148	(-0.6)		
Zeng (Ref. 19)			2.294	(6.1)	2.300	(6.4)		
FP (Ref. 20)								
Expt. (Ref. 67)	2.162							

TABLE VI. The computed bulk moduli (in GPa) and their derivatives (in parentheses) of pyrite.

Method	LDA		GGA		B3LYP	
CASTEP	208	(4.4)	164	(5.2)		
CRYSTAL98	209	(7.9)	164	(3.5)	113	(5.7)
Expt.	143 (4, assumed) 54 148 (5.5) 55 157 (-) 56 215 (5.5) 57					

and B3LYP treatments of exchange and correlation all yielding structural parameters in reasonable agreement with experiment. The CRYSTAL98 and CASTEP calculations performed within the LDA overestimate binding energy, leading to an underestimate in the cell volumes. GGA functionals correct for the overbinding and result in increased cell volumes by about 2%. The differences in the cell parameter computed using CRYSTAL98 and CASTEP is probably due to the use of the pseudopotential approximation in CASTEP whereas in CRYSTAL98 an all electron basis set was used throughout. Other GGA studies using the VASP[53] plane wave code with different computational parameters and parametrization of the Ultrasoft pseudopotential gave slightly different lattice parameters (1.1% for a_0, 0.25% for x_s) compared to the current CASTEP results.

The HF approximation fails to predict accurate structural parameters due to the nature of the spin on the Fe ions. Since pyrite is diamagnetic, the Fe^{2+} ions are in a low-spin configuration with fully occupied t_{2g} and empty e_g states. Electron correlation effects will tend to reduce the electron–electron repulsion in the fully occupied orbitals leading to an increase in the binding of the electrons in these states. This results in a decrease in the Fe^{2+} ionic radius and hence a smaller lattice cell length. It seems likely that the complete neglect of correlation effects in HF theory would contribute to the large overestimate of the cell parameter with respect to experiment. To test this hypothesis, we have performed supplementary geometry optimizations using HF theory with *a posteriori* correlation corrections. We find that the addition of correlation effects, even at such a crude level, leads to a significant reduction in the overestimate of the cell parameter (5.89 Å with correlation corrections, 6.00 Å uncorrected). Similarly, structural optimizations performed at the LDA level of theory but without computing the correlation energy results in an increase in the cell parameter (5.470 Å, compared to 5.386 Å with correlation). Our calculations also revealed that the LDA, GGA and B3LYP methods give low-spin (diamagnetic) solutions as the ground state of pyrite, with computed total energies which are lower than the high-spin (paramagnetic) state by 17, 12.3 and 3.9 eV, respectively, while Hartree–Fock theory predicts the high-spin state to be more stable by 2 eV. This erroneous prediction is due to the lack of correlation in HF theory, as discussed in Sec. III. The ''pure DFT'' methods incorporate correlation to some extent, resulting in improved calculated structural parameters and the correct prediction of spin state. The value of the energy of the low-spin state relative to the high-spin state acquired using B3LYP is in line with expectations; since the B3LYP functional is a linear combination of HF and GGA, it is not unreasonable to expect it to give a value which lies between those acquired using these two methods, i.e., -3.9 eV obtained from B3LYP lies between -12.3 eV (GGA) and $+2$ eV (HF).

In the current study, B3LYP calculations of the band gap of pyrite predict a value of around 2 eV. The experimental value, determined using a number of different techniques has been measured to be between 0.7 and 2.62 eV, with the most reliable values (0.9 to 0.95 eV) coming from photoconductivity measurements.[58] As the B3LYP calculations are of the ground state of the system, a disagreement with respect to experiment is not surprising. However, a recent study has showed that calculations using the B3LYP treatment of exchange and correlation give predictions of the band gap of a wide range of minerals with an accuracy comparable to that of far more computationally expensive quantum Monte Carlo simulations.[36]

Considering the findings reported in Ref. 36, it seems surprising that B3LYP overstimates the band gap of pyrite by a factor of 2. However, the overestimate of the band gap may be understood by considering the influence that defects would have on the real crystal. Spectroscopic studies have probed the defect nature of natural and synthetic pyrite.[59] Luck[59] found that pyrite crystals are exclusively sulphur deficient, with the empirical formula better expressed as FeS_{2-x} with x ranging from 0.05 to 0.25. Birkholz *et al.*[60] used ligand field theory arguments to suggest that the 5-fold (tetragonal pyramidial) coordinated Fe ions resulting from sulphur vacancies would have a modified splitting of the Fe 3d orbitals compared to the 6-fold (octahedrally) coordinated, stoichiometric Fe ions. The crystal field splitting in the 5-coordinate Fe ions would result in the formation of new defect states lying between the valence and conduction bands and would lead to a reduction in the measured band gap, and as such may account for the discrepancy between the calculated and experimentally measured values.

Other features of the densities of states computed using CRYSTAL98 are in excellent agreement with experiment. The splitting of the S 3s states has been attributed to the formation of bonding (σ_b) and antibonding (σ_a) states arising from overlap between sulphur nearest neighbors. The degree of overlap and hence the gap between the states is dependent on the S–S bond distance. In Fig. 5, we show the DOS computed using the LDA for a range of S–S bond distances from 2.66 Å ($x_s = 0.358$) to 1.91 Å ($x_s = 0.398$) at the optimized LDA cell volume. The S–S bond distance has been varied by changing the internal coordinate of the S ions. The effect of changing this bond distance on the splitting of the S states is dramatic. The gap between the σ_b and σ_a varies from 5 eV at 1.91 Å to about 0.5 eV at 2.47 Å with the gap disappearing at larger separations. We note that our LDA calculations of the DOS at the x_s parameter as computed

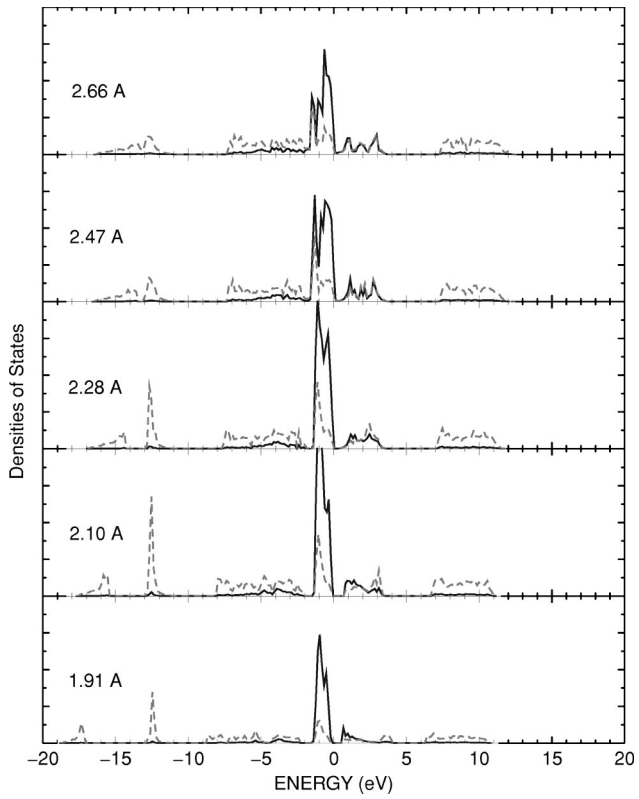

FIG. 5. The influence of the S–S bond distance on the S 3s bonding and antibonding peak positions computed using CRYSTAL98 within the LDA.

using CRYSTAL98 or CASTEP yields a conducting state for both methods although the predicted value of x_s varies somewhat (CRYSTAL, 0.378, CASTEP 0.382). We have performed tests, computing the DOS using CRYSTAL98 at $x_s = 0.382$ and find a conducting state.

The influence of the lattice parameters, a_0 and x_s on the pyrite band structure were determined by calculation of the density of states and band structure at a series of applied isotropic pressures ranging from −15 GPa to +20 GPa (see Fig. 6) using B3LYP. Note that in this case ''negative'' applied isotropic pressures are fictitious quantities, and simply cause the cell volume to increase with respect to the calculated cell volume at 0 GPa. Both a_0 and x_s were found to decrease with increasing pressure (see Fig. 7). While both Fe–S and S–S bond distances decrease with pressure, Fe–S bonds were found to compress more readily than S–S bonds, in agreement with the calculations of Opahle *et al.*[20] As a consequence, the unit cell also decreases in volume more rapidly with pressure than S–S bond distances. However, at higher applied pressures, the rate of compression of Fe–S and S–S bonds becomes increasingly similar (see Fig. 8) since, in general, as bond lengths are decreased, the energetics of compression are increasingly dominated by the repulsive component of their interaction curves. Changes in the pyrite structure with pressure have several significant effects on the band structure (see Fig. 9). In general, there is an increased dispersion of bands with pressure, as expected, due to the enhanced coupling between adjacent unit cells which arises from a decrease in cell volume. It was also found that occupied bands are lowered in energy with respect to the valence band maximum (VBM), while the energies of unoccupied bands are raised. These effects are attributed to enhanced covalency between Fe and S as the Fe–S bond distance is decreased. The formation of a steep band (shown in bold in Fig. 9) at the Γ point was found at around 0 GPa, which becomes the conduction band minimum (CBM) at pressures greater than 0 GPa. At the Γ point, this band lowers in energy with respect to the VBM with increasing pressure, causing reduction of the band gap. Thus, in terms of the lattice parameters, a decrease in x_s causes reduction in the band gap due to lowering of the CBM at the Γ point. This behavior may be explained in terms of interactions between S_2 dimers in the pyrite ''sub-lattice'' model, given by Eyert *et al.*[48] The band at CBM is predominantly S 3p in character, and is directly related to the S–S bond distance. According to Eyert, at constant cell volume, decrease in x_s (increase in

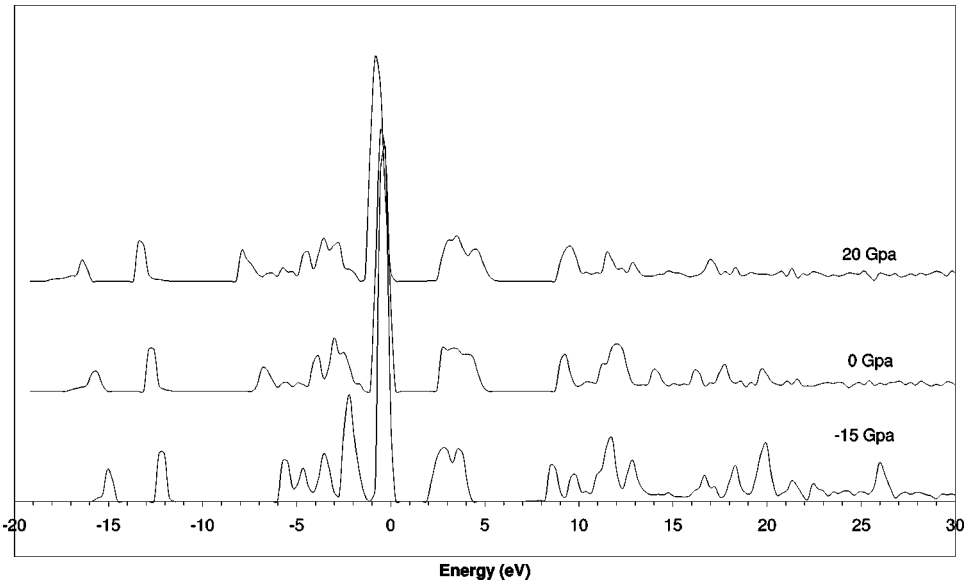

FIG. 6. The total densities of states for FeS_2 computed using B3LYP at a range of pressures.

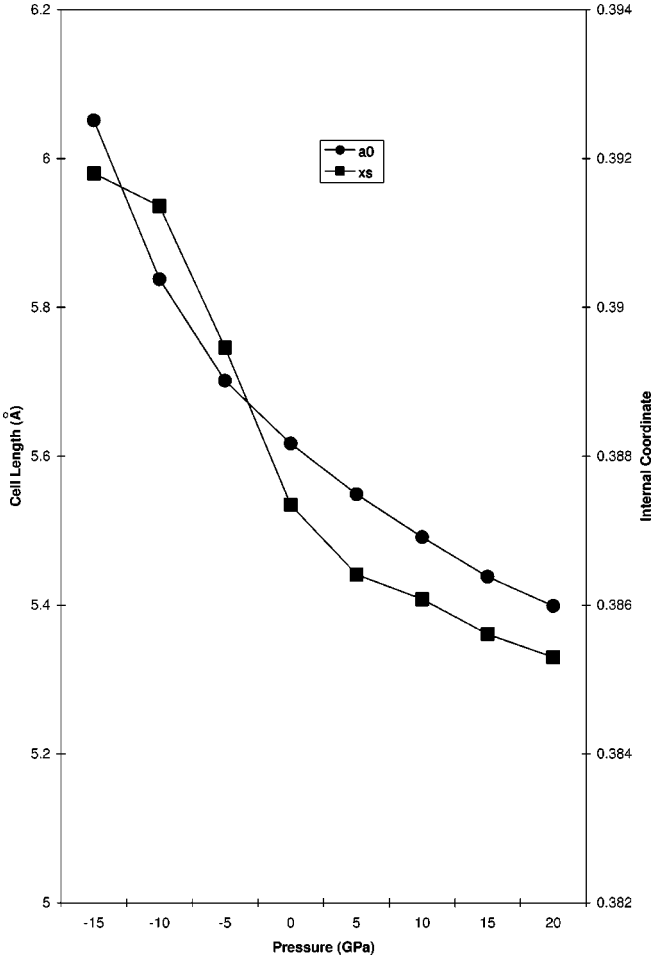

FIG. 7. The cell parameters of FeS_2 at various pressures as computed using B3LYP.

S–S bond length) causes increased coupling between S_2 dimers, resulting in increased band dispersion at the CBM. Our results show that there is a decrease in S–S bond length with increasing pressure. However, as explained above, since the Fe–S bonds compress more readily than S–S bonds, the cell volume decreases more rapidly than S–S bond lengths with pressure. Thus there is an overall increased coupling between S_2 dimers, leading to increased dispersion of S 3p

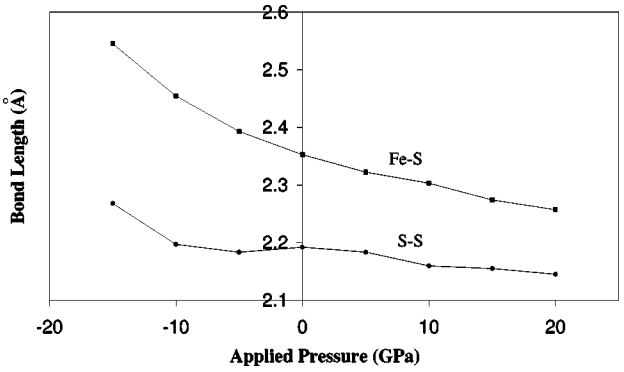

FIG. 8. The change of Fe–S and S–S bond lengths with applied pressure as computed using B3LYP.

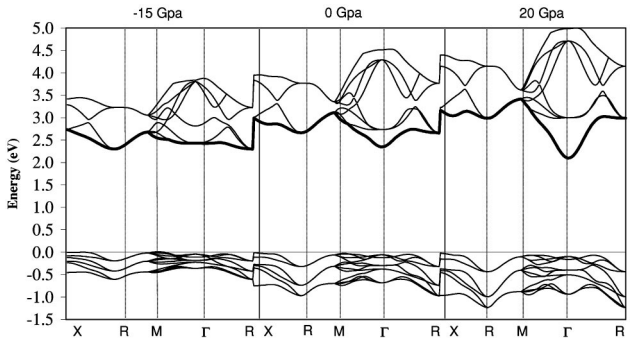

FIG. 9. The influence of pressure on the band structure of FeS_2 computed using CRYSTAL98 with the B3LYP functional.

band at the Γ point and a lowering of the CBM. Note that this result is contrary to the expectations pointed out by Eyert *et al.*,[48] but is consistent with the calculations of Opahle *et al.*[20] The rate of energy lowering of the CBM slows at higher pressures, since the Fe–S bonds (and hence cell volume) and S–S bonds compress at more similar rates at higher pressures, leading to a lower rate of increase in interactions between S_2 dimers. Although our results show that the band gap decreases with applied pressure, the blue shift of the optical band gap that is observed experimentally may be explained by considering the DOS. The band at the Γ point that causes the band gap reduction only contributes to a very shallow tail in the DOS (see Figs. 6 and 9) in agreement to earlier studies,[20] while the antibonding Fe 3d and S 3p states immediately above this band are raised in energy with respect to increasing pressure VBM. Neglecting the steep band at the CBM, our calculations predict an optical blue shift of around 0.016 eV per GPa of pressure applied, in excellent agreement with the value of around 0.02 eV per GPa obtained by Batlogg *et al.*[61,62] from pressure experiments. Our results therefore suggest that this band may be neglected in interpretation of the optical phenomena of pyrite.

We have investigated possible causes for the poor description of the S–S bond length by the CRYSTAL98 calculations. Comparing the S–S bond distance computed using basis sets with and without d-symmetry polarization functions on the sulphur ions, we find that the lack of polarization functions results in an increase in the S–S distance of up to 9% relative to the S–S distance computed with polarization functions. Clearly, polarization functions are very important in describing the S–S bond. To examine these effects further, we have performed additional tests using the GAUSSIAN98 code[63] to determine how important d-symmetry and higher angular momentum polarization functions are in describing S_2 molecules and S_2^{2-} dimers. These calculations were performed using the 6-311+G basis set which does not include any polarization functions, the 6-311+G(d) basis which includes one d-symmetry function on each sulphur atom and, finally, the 6-311+G(3df) basis set which includes three d-symmetry functions and an additional f-symmetry function. Although the systems modeled by the Gaussian calculations were in the gas phase, the results, shown in Table VII, illustrate that d-symmetry functions are essential for a reasonable descrip-

TABLE VII. Bond distances computed for S_2 dimers in Å. The CRYSTAL98 results relate to the S–S bond distance computed in pyrite whereas the Gaussian data are for S_2 and S_2^{2-} dimers in the gas phase.

Method	Basis set	HF	LDA	GGA	B3LYP
		S_2^{2-} bond distance in FeS_2			
CRYSTAL98	no d	2.196	2.422	2.461	2.386
	d	2.143	2.274	2.295	2.197
Experiment	2.162 (Ref. 67)				
		S_2^{2-} dimer			
GAUSSIAN98	6-311+G	2.329	2.352	2.384	2.388
	6-311+G(d)	2.180	2.191	2.225	2.231
	6-311+G(3df)	2.153	2.133	2.170	2.181
		S_2 dimer			
GAUSSIAN98	6-311+G	2.017	2.069	2.083	2.073
	6-311+G(d)	1.879	1.922	1.937	1.927
	6-311+G(3df)	1.863	1.897	1.911	1.903
Experiment	1.887 (Ref. 68)				

tion of the S_2 and S_2^{2-} dimers and that f-symmetry polarization functions may be necessary to fully converge the bond distances with respect to the basis set. However, as discussed in Sec. II, basis functions with f- or g-symmetry are not available in the CRYSTAL98 code. This may also explain part of the discrepancy between the CRYSTAL98 and CASTEP results.

V. CONCLUSIONS

In the current study, we have performed calculations on FeS_2 using a variety of theoretical treatments, in particular, HF, DFT and hybrid-functional treatments of exchange and correlation, and computational approaches using the all-electron LCAO technique and the plane wave pseudopotential methodology.

The computed results are influenced by the selection of the treatment of exchange and correlation. Correlation effects must be taken into account in order to yield the correct electronic ground state and structrual parameters. The HF approximation provides a poor description of pyrite FeS_2 giving an incorrect ground state. In contrast, calculations performed with DFT and hybrid-functional (B3LYP) methods provide a reasonable description of FeS_2. Calculations performed within the LDA generally underestimate the cell volume whereas GGA corrects for this effect. The tests in the current study reveal that sulphur undergoes significant polarization effects. Calculations performed using atomic-orbital basis sets must take account for these effects and include higher angular momentum polarization functions.

The current DFT and B3LYP calculations give a good description of the occupied electronic states. The position and width of the valence bands are in good agreement with experiment. However, LDA and GGA underestimate the band gap and predict pyrite to be a conductor. B3LYP calculations yield a band gap of about 2 eV, significantly larger than the accepted experimental value of 1 eV. We believe that a possible reason for the discrepancy is due to the fact that experimentally, pyrite is usually sulphur deficient and can be better described by the formula FeS_{2-x} where x can vary from 0.05 to 0.25. This large deviation from ideal stoichiometry leads to the formation of new defect states within the band gap and may give rise to the low experimentally determined value.

The current study provides an understanding of how different computational methodologies affect the description of the structural and electronic properties of FeS_2 and serves to underpin further studies of the surface structure and chemistry of pyrite FeS_2.

ACKNOWLEDGMENTS

We thank Accelrys Inc. for provision of a CASTEP license during this study and to Professor Stephen Fletcher (University of Loughborough) for initiating the collaboration between CSIRO Minerals and RMIT. The calculations were performed on Silicon Graphics workstations and a parallel PC cluster.[64]

[1] N. Weiss, Ed., *SME Mineral Processing Handbook* (Society of Mining Engineers, New York, 1985).

[2] A. Ennaoui, S. Fiechter, W. Jaegermann, and H. Tributsch, J. Electrochem. Soc. **133**, 97 (1986).

[3] S. S. Wang and R. N. Seefurth, J. Electrochem. Soc. **134**, 530 (1987).

[4] R. T. Shuey, *Semiconducting Ore Minerals* (Elsevier, Amsterdam, 1975).

[5] D. K. Nordstrom, *Acid Sulphate Weathering, Spec. Pub. No. 10* (Soil Sci. Soc. Amer., Madison, WI, 1982).
[6] K. Laajalehto, I. Kartio, and E. Suoninen, Int. J. Min. Process. **51**, 163 (1997).
[7] H. van der Heide, R. Hemmel, C. F. van Bruggen, and C. Haas, J. Solid State Chem. **33**, 17 (1980).
[8] K. M. Rosso, U. Becker, and M. F. Hochella, Jr., Am. Mineral. **84**, 1535 (1999).
[9] T. Ollonqvist, R. Perala, and J. Vayrynen, Surf. Sci. **377-379**, 201 (1997).
[10] E. Puppin, M. Finazzi, and F. Ciccacci, Solid State Commun. **82**, 489 (1992).
[11] A. K. Abass, Z. A. Ahmed, and R. E. Tahir, J. Appl. Phys. **61**, 2339 (1987).
[12] A. Pasquarello, M. S. Hybertsen, and R. Car, Nature (London) **396**, 58 (1998).
[13] P. J. D. Lindan, N. M. Harrison, and M. J. Gillan, Phys. Rev. Lett. **80**, 762 (1998).
[14] A. Vittadini, A. Selloni, F. P. Rotzinger, and M. Gratzel, Phys. Rev. Lett. **81**, 2954 (1998).
[15] K. C. Hass, W. F. Schneider, A. Curioni, and W. Andreoni, Science **282**, 265 (1998).
[16] D. W. Bullet, J. Phys. C **15**, 6163 (1982).
[17] W. M. Temmerman, P. J. Durham, and D. J. Vaughan, Phys. Chem. Miner. **20**, 248 (1993).
[18] D. Nguyen-Manh, D. G. Pettifor, H. M. Sithole, P. E. Ngoepe, C. Arcangeni, R. Tank, and O. Jepsen, Mater. Res. Soc. Symp. Proc. **491**, 401 (1998).
[19] Y. Zeng and N. A. W. Holzwarth, Phys. Rev. B **50**, 8214 (1994).
[20] I. Opahle, K. Koepernik, and H. Eschrig, Phys. Rev. B **60**, 14 035 (1999).
[21] H. M. Sithole, D. Nguyen-Manh, D. G. Pettifor, and P. E. Ngoepe, Mol. Simul. **22**, 31 (1999).
[22] V. R. Saunders, R. Dovesi, C. Roetti, M. Causà, N. M. Harrison, R. Orlando, E. Aprà, and C. M. Zicovich-Wilson, CRYSTAL95 *User's Manual* (University of Turin, Turin, 1996).
[23] M. C. Payne, M. P. Teter, D. C. Allan, T. A. Arias, and J. D. Joannopoulos, Rev. Mod. Phys. **64**, 1045 (1992).
[24] http://www.dl.ac.uk/TCS/Software/CRYSTAL/ (The CRYSTAL Basis set library, Daresbury, UK, 1998).
[25] M. Mian, N. M. Harrison, V. R. Saunders, and W. R. Flavell, Chem. Phys. Lett. **257**, 627 (1996).
[26] A. D. Becke, J. Chem. Phys. **98**, 5648 (1993).
[27] W. Kohn and L. J. Sham, Phys. Rev. **140**, A1133 (1965).
[28] D. M. Ceperley and B. J. Alder, Phys. Rev. Lett. **45**, 566 (1980).
[29] J. P. Perdew and A. Zunger, Phys. Rev. B **23**, 5048 (1981).
[30] J. P. Perdew, K. Burke, and M. Ernzerhof, ACS Symp. Ser. **629**, 453 (1996).
[31] J. P. Perdew, K. Burke, and M. Ernzerhof, Phys. Rev. Lett. **77**, 3865 (1996).
[32] P. J. Stephens, F. J. Devlin, C. F. Chabalowski, and M. J. Frisch, J. Phys. Chem. **98**, 11 623 (1994).
[33] A. D. Becke, Phys. Rev. A **38**, 3098 (1988).
[34] C. Lee, W. Yang, and R. G. Parr, Phys. Rev. B **37**, 785 (1988).
[35] S. H. Vosko, L. Wilk, and M. Nusair, Can. J. Phys. **58**, 1200 (1980).
[36] J. Muscat, A. Wander, and N. M. Harrison, Chem. Phys. Lett. **342**, 397 (2001).
[37] J. D. Pack and H. J. Monkhorst, Phys. Rev. B **16**, 1748 (1977).
[38] C. Pisani, R. Dovesi, and C. Roetti, *Hartree–Fock Ab Initio Treatment of Crystaline Systems* (Springer-Verlag, Berlin, 1988), Vol. 48.
[39] R. Dovesi, C. Roetti, C. Freyria-Fava, E. Aprà, V. R. Saunders, and N. M. Harrison, Philos. Trans. R. Soc. London, Ser. A **341**, 203 (1992).
[40] C. Zhu, R. H. Byrd, P. Lu, and J. Nocedal, *L-BFGS-B—Fortran Subroutines for Large Scale Bound Constrained Optimization* (Department of Electrical Engineering and Computer Science, Northwestern University, 1994).
[41] J. P. Perdew, J. A. Chevary, S. H. Vosko, K. A. Jackson, M. R. Pederson, D. J. Singh, and C. Fiolhais, Phys. Rev. B **46**, 6671 (1992).
[42] D. Vanderbilt, Phys. Rev. B **41**, 7892 (1990).
[43] N. Troullier and J. L. Martins, Phys. Rev. B **43**, 1993 (1991).
[44] F. D. Murnaghan, Proc. Natl. Acad. Sci. U.S.A. **30**, 244 (1944).
[45] S. Miyahara and T. Teranishi, J. Appl. Phys. **39**, 896 (1968).
[46] R. S. Mulliken, J. Chem. Phys. **23**, 1833 (1955).
[47] J. Muscat, Ph.D. thesis, University of Manchester, Manchester, 1999.
[48] V. Eyert, K.-H. Hoeck, S. Fiechter, and H. Tributsch, Phys. Rev. B **57**, 6350 (1998).
[49] W. Folkerts, G. A. Sawatzky, C. Haas, R. A. Degroot, and F. U. Hillebrecht, J. Phys. C **20**, 4135 (1987).
[50] J. Muscat and C. Klauber, Surf. Sci. **491**, 226 (2001).
[51] Y-M. Juan and E. Kaxiras, Phys. Rev. B **48**, 14 944 (1993).
[52] A. Hung, I. Yarovsky, J. Muscat, S. Russo, and I. Snook, Surf. Sci. (in press).
[53] P. Raybaud, J. Hafner, G. Kresse, and H. Toulhoat, J. Phys.: Condens. Matter **9**, 11 085 (1997).
[54] A. Jephcoat and P. Olson, Nature (London) **325**, 332 (1987).
[55] H. G. Drickamer, R. W. Lynch, R. L. Clendenen, and E. A. Perez-Albuerne, Solid State Phys. **19**, 135 (1966).
[56] T. Fujii, A. Yoshida, K. Tanaka, F. Marumo, and Y. Noda, Mineral. J. **13**, 202 (1986).
[57] T. Chattopadhyay and H. G. von Schnering, J. Phys. Chem. Solids **46**, 113 (1985).
[58] A. Ennaoui, S. Fiechter, C. Pettenkofer, N. Alonso-Vante, K. Buker, M. Bronold, C. Hoepfner, and H. Tributsch, So. Energy Mater. Sol. Cells **29**, 289 (1993).
[59] J. Luck, A. Hartmann, and S. Fiechter, Fresen. Z. Anal. Chem. **334**, 441 (1989).
[60] M. Birkholz, S. Fiechter, A. Hartmann, and H. Tributsch, Phys. Rev. B **43**, 11 926 (1991).
[61] A. Schlegel and P. Wachter, J. Phys. C **9**, 3363 (1976).
[62] B. Batlogg (private communication).
[63] M. J. Frisch, G. W. Trucks, H. B. Schlegel, G. E. Scuseria, M. A. Robb, J. R. Cheeseman, V. G. Zakrzewski, J. A. Montgomery, Jr., R. E. Stratmann, J. C. Burant, S. Dapprich, J. M. Millam, A. D. Daniels, K. N. Kudin, M. C. Strain, O. Farkas, J. Tomasi, V. Barone, M. Cossi, R. Cammi, B. Mennucci, C. Pomelli, C. Adamo, S. Clifford, J. Ochterski, G. A. Petersson, P. Y. Ayala, Q. Cui, K. Morokuma, D. K. Malick, A. D. Rabuck, K. Raghavachari, J. B. Foresman, J. Cioslowski, J. V. Ortiz, A. G. Baboul, B. B. Stefanov, G. Liu, A. Liashenko, P. Piskorz, I. Komaromi, R. Gomperts, R. L. Martin, D. J. Fox, T. Keith, M. A. Al-Laham, C. Y. Peng, A. Nanayakkara, C. Gonzalez, M. Challacombe, P. M. W. Gill, B. Johnson, W. Chen, M. W. Wong, J. L. Andres, C. Gonzalez, M. Head-Gordon, E. S. Replogle, and J. A. Pople, *Gaussian 98, Revision A.7* (Gaussian, Inc., Pittsburgh, PA, 1998).

[64] J. Muscat and W. Burrage, *Low Cost Unix Type Multiprocessing System* (CSIRO Minerals, DMR No. 1684, Melbourne, 1999).
[65] A. G. Schaufuss, H. W. Nesbitt, I. Kartio, K. Laajalehto, G. M. Bancroft, and R. Szargan, Surf. Sci. **411**, 321 (1998).
[66] H. W. Nesbitt, G. M. Bancroft, A. R. Pratt, and M. J. Scaini, Am. Mineral. **83**, 1067 (1998).
[67] S. Finklea, L. Cathey, and E. Amma, Acta Crystallogr., Sect. A: Cryst. Phys., Diffr., Theor. Gen. Crystallogr. **32**, 529 (1976).
[68] L. E. Sutton, Ed., *Interatomic Distances Supplement, Special Publication No. 18* (The Chemical Society, London, 1965).